



In-process phased array ultrasonic weld pool monitoring

Nina E. Sweeney^{a,b,*}, Simon Parke^b, David Lines^a, Charalampos Loukas^a, Momchil Vasilev^a, Stephen G. Pierce^a, Charles N. MacLeod^a

^a Centre for Ultrasonic Engineering (CUE), Department of Electronic & Electrical Engineering, University of Strathclyde, Glasgow G1 1XQ, UK

^b Peak NDT Ltd, Jubilee Business Park, 1 Enterprise Way, Derby DE21 4BB, UK



ARTICLE INFO

Keywords:

Weld pool monitoring
Phased array ultrasonics
In-process
Welding
Non-destructive testing

ABSTRACT

In recent years, there have been increasing economic and industrial drivers for the development of real-time non-destructive evaluation directly at the point of manufacture. Real-time inspection and monitoring of welding processes can help to reduce fabrication costs by detecting defects as they occur, enabling more efficient and cost-effective builds. This paper shows, for the first time, the use of phased array ultrasonics to monitor and analyse the molten weld pool during deposition of multi-pass gas tungsten arc welds. The received ultrasonic signals are shown to contain information related to key physical transitions occurring within the welding process, namely the melting and solidification of the weldment. Furthermore, the technique used here is shown to be effective for determining weld quality in real-time with significant signal changes occurring when defects such as Lack of Root Penetration are present. The accurate focusing and steering capabilities offered by phased arrays are used to successfully isolate the molten weld pool from the surrounding solidified weldment during deposition of multiple layers of a multi-pass weld.

1. Introduction

Many industrial sectors, such as energy and defence, employ Non-Destructive Evaluation (NDE) as a means of ensuring the integrity of welded components at manufacture and throughout their service life. Often, these welded components are composed of thick sections which necessitate the need for high-integrity welding processes with multi-pass weld deposition strategies. As a general rule, NDE of multi-pass welds occurs as a final step in the manufacturing timeline, on the cold component and once a sufficient time period has lapsed so as to detect delayed defects, such as hydrogen cracking, in accordance with international testing standards [1,2]. This greatly complicates the rework procedure, resulting in increased cost, particularly where defects are present in early weld runs, as a significant amount of work is required to excavate the defective area before repair and retesting. Recently, there have been increasing industrial and economic drivers to reduce manufacturing costs, particularly as the energy sector is being called upon to play a significant role in the delivery of low-carbon energy production in the future [3]. The application of innovative in-process inspection and monitoring techniques is one way in which the NDE sector can support the achievement of this aim. In-process monitoring

and inspection of welding processes makes it possible to detect the formation of defects at the earliest possible point to enable quicker and more cost-effective repair while improving manufacturing schedule certainty. Furthermore, the valuable data gathered through in-process monitoring of welding processes may be used to control and optimise the process in real-time to reduce the overall rate of defect formation.

It has previously been discussed that the two most important information sources which require monitoring to help ensure weld quality in-process are the weld seam and the weld pool [4]. While weld seam tracking has been successfully deployed using laser and active vision systems [5–7] and arc sensing technologies [7,8], developments in effective weld pool sensing have yet to be delivered.

Currently, the most widely adopted methods for monitoring the weld pool use passive vision through specialised High Dynamic Range (HDR) cameras [9–11]. Vision systems can be used for the measurement of weld pool width, length and, in some cases, surface convexity which can be used to predict penetration depth [12]. Infrared (IR) cameras have been used to monitor the temperature of molten weld pools which can also be related to the penetration depth [13,14]. Visual methods only provide external surface measurements with no indication of the internal structure of the weld pool and predictions must be made to infer

* Corresponding author. Centre for Ultrasonic Engineering (CUE), Department of Electronic & Electrical Engineering, University of Strathclyde, Glasgow, G1 1XQ, UK.

E-mail address: nina.sweeney@strath.ac.uk (N.E. Sweeney).

other important geometrical properties which cannot be measured directly i.e. penetration depth. Furthermore, the requirement for a direct line of sight to the weld pool makes them inappropriate for use in conjunction with many geometries and welding processes such as Submerged Arc Welding (SAW).

The most common methods available which can provide volumetric and internal weld pool information are Radiographic Testing (RT), Eddy Current Testing (ECT) and Ultrasonic Testing (UT). RT has limitations in terms of applicability on thicker materials [15] and the need for radiation safety management [16]. The use of ECT for inspection is limited by the achievable penetration depth [17]. Ultrasonic sensing technologies in the field of weld pool monitoring has not been widely adopted, however, it has become a key area of research in recent years.

An in-line approach for real-time monitoring of the Resistive Spot Welding (RSW) process using ultrasonics has been successfully implemented within commercial spot welding equipment [18,19]. Here, pulse-echo ultrasonic inspection is used to monitor the growth and solidification of spot welds. Through characterisation of the resultant signal responses, an effective screening method for spot-welds was developed which can identify spot welds with insufficient penetration [20,21]. The application of linear and matrix arrays to provide additional information in this area has also been explored [22,23].

Air-coupled ultrasonics have also been used successfully for in-process screening of thin section butt welds, through the use of guided Lamb waves [24]. While air-coupled ultrasonics has the advantage of being non-contact in a high-temperature environment, the Signal-to-Noise Ratio (SNR) is generally low when compared with traditional contact alternatives [25]. Laser ultrasonics, another non-contact approach, has also been used to monitor the joining of lapped steel plates using fusion Gas Tungsten Arc Welding (GTAW) spot welding [26]. Laser ultrasonic generation has also been used alongside Electro Magnetic Acoustic Transducers (EMATs) for reception to estimate the penetration depth of a fusion butt weld in real-time [27]. Laser ultrasonic systems come with stringent safety requirements for in-situ deployment and are currently far more expensive to implement than conventional UT systems [28].

Real-time ultrasonic thickness measurements have been used to provide a priori knowledge of material thickness in order to inform a feed-forward closed-loop control system capable of welding butt joints of varying thickness while maintaining consistent penetration [29]. This indirect sensing method does not provide information relating to the weld pool itself and instead relates the thickness measurement to appropriate welding parameters based on a pre-defined parametric function. Traditional single-element contact ultrasonics has been used successfully to monitor in real-time the deposition of the root pass of a multi-pass gas tungsten arc weld [30]. The use of longitudinal ultrasonic waves in an angled beam pitch-catch setup was shown to be effective in monitoring and characterising the weld pool. Furthermore, this technique also showed promise for the detection of defects as they are formed. However, significant limitations of this approach are anticipated when considering its use for monitoring higher passes within a multi-pass weld. Single-element transducers have fixed physical characteristics which constrain their operation, such as natural focus and beam spread [31]. Furthermore, angled inspections are limited to pre-defined individual angles through the use of wedges. Focusing of the ultrasonic energy at different angles and positions is a necessity for accurate isolation of the weld pool from the surrounding solidified material. Phased Array Ultrasonic Testing (PAUT) has become increasingly popular in many NDE applications over recent years, due to the arrays flexibility when compared with single-element transducers [32]. They offer the ability to implement a large number of inspection modalities with a single transducer from a single inspection point, increasing coverage and sensitivity [33] and making them a more appropriate choice.

In this body of work, phased array ultrasonic testing is used to interrogate the molten weld pool in real-time. The benefit of using

phased arrays rather than single-element equipment is explored as well as the unavoidable effects that the temperature gradients introduced during welding have on ultrasonic transit times and direction. Longitudinal wave modes were used in a focused pitch-catch arrangement to monitor the deposition of both root and hot pass welds. It has been determined from these investigations that sufficient information can be extracted from the ultrasonic signals to isolate the molten weld pool and monitor the deposition of multi-pass welds in-process. It is also deemed that the information held within the ultrasonic signals is of sufficient quality to inform process control algorithms in the future.

2. Technical background

2.1. Single-element vs. phased array ultrasonic testing

The inspection of individual weld passes within a multi-pass weld, as necessary for in-process monitoring of the weld pool, is effectively impossible using single-element transducers due to their aforementioned limitations. As the weld cross-section is filled, it becomes increasingly difficult to isolate the liquid weld pool from the already deposited and solidified weld material surrounding it. Due to the effects of beam spread, the acoustic energy propagates into the surrounding solid material, obscuring any signals from the molten weld pool due to acoustic velocity differences and attenuation. Phased arrays are therefore an attractive alternative in this scenario, allowing accurate beam steering and focusing to concentrate the ultrasonic energy on the intended molten weld pool. Furthermore, through the use of angular sweeps, additional data for optimisation purposes can be collected within a single acquisition.

Fig. 1 shows models produced using the NDT simulation software package CIVA [34] of a weld inspection using (a) an unfocused longitudinal transmission using a 6 mm diameter single-element probe with a 70° wedge and (b) a phased array 70° longitudinal transmission focused at the root. The approximate welding pass layout has been overlaid in each case. The focusing capabilities of the phased array inspection allow for more accurate isolation of individual passes. In the case of the single-element inspection, the natural focus of the probe means that the beam energy is concentrated not far below the surface of the specimen and the associated beam spread results in a large area of the weld being covered. While the beam spread and natural focus of a single-element probe can be altered by design, a bespoke set of probes and wedges would be needed for each weld pass which quickly becomes impractical when considering varying geometries and welding pass sequences. Through the correct provision of angle and focus point, the phased array can maximise the amount of energy transmitted through a single weld pass.

2.2. Temperature considerations

The effect of temperature on ultrasonic parameters such as acoustic velocity, attenuation and angle of refraction is well documented [35,36] along with the challenges these effects pose for in-process weld inspection [37,38]. The thermal gradients created during the welding process are extreme and the subsequent beam bending effects due to refraction have a significant influence on the position and amplitude of defect signals received during traditional ultrasonic testing. The complex beam refraction taking place through these thermal gradients makes it challenging to predict the true direction of sound propagation within the component. Furthermore, conventional ultrasonic contact probes are incapable of operating in these high-temperature environments, with a maximum operating temperature of ~60 °C, necessitating the development of alternatives [39,40].

Fig. 2 shows cross-sections, in a plane perpendicular to the weld torch travel, taken from experimentally validated thermal simulations of a GTAW process applied to a multi-pass weld on carbon steel S275. In **Fig. 2a** the slice is taken from the plane directly beneath the welding

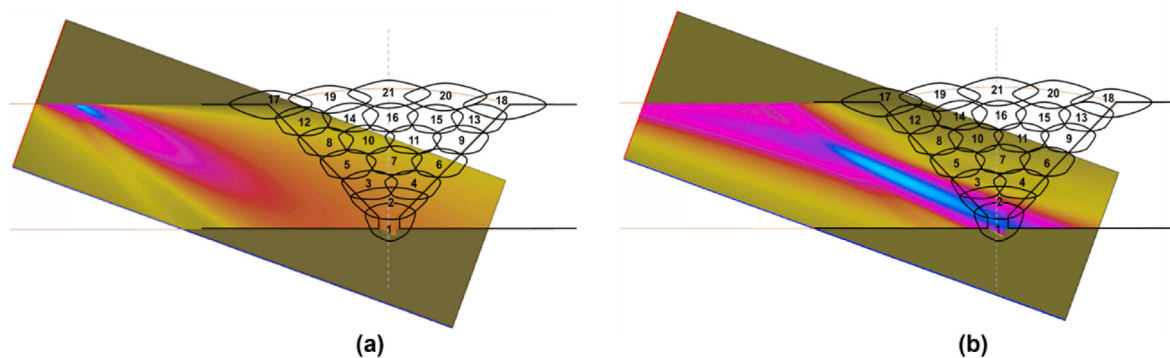


Fig. 1. CIVA beam computation models of a 70° weld inspection using (a) an unfocused single-element probe and (b) a focused phased array probe with weld pass overlays.

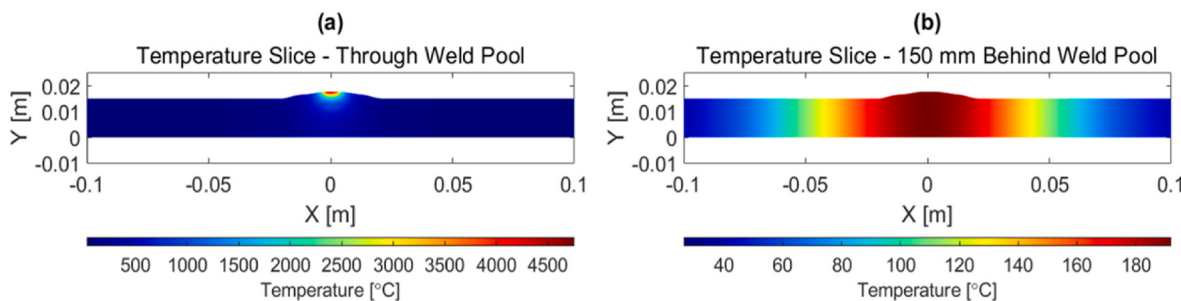


Fig. 2. Experimentally validated COMSOL results of temperature gradients created during welding with cross-sections taken through planes (a) in-line with the welding heat source and (b) 150 mm behind the weld pool.

heat source, while Fig. 2b shows a slice taken 150 mm behind the weld torch. Clearly, the thermal gradients experienced will be greatest where the ultrasonic probes are in-line with the weld torch, imaging the weld pool directly. Compensation strategies are currently being developed

[38] to account for the variations and uncertainty caused by thermal gradients.

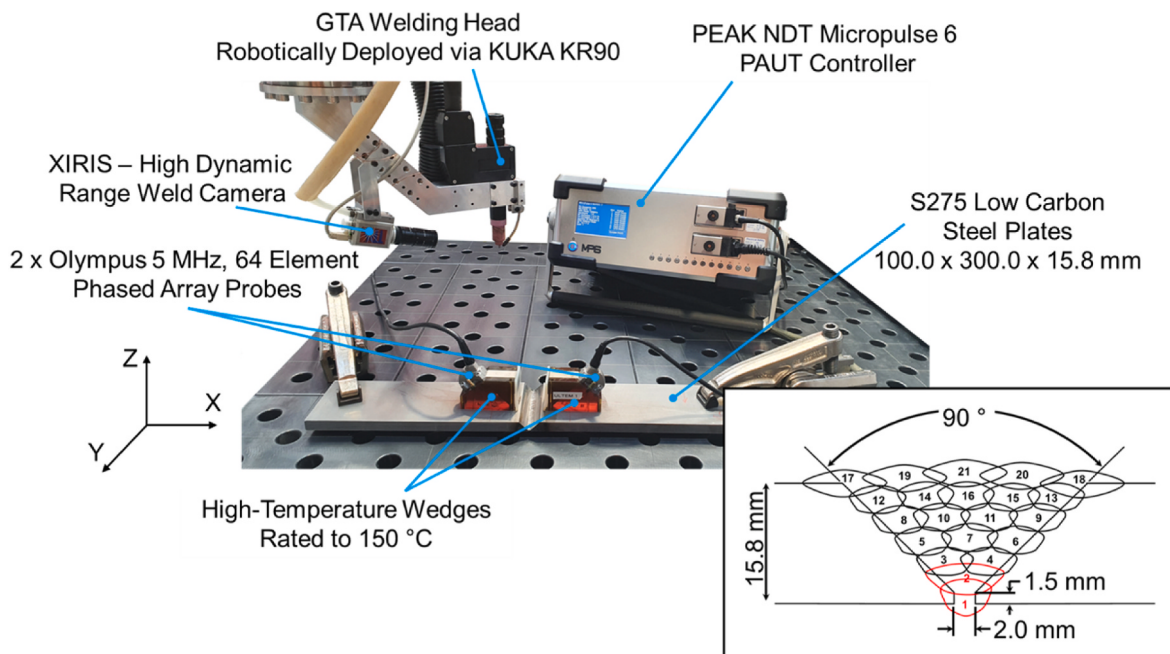


Fig. 3. Experimental hardware set up. A 6 DOF robotic manipulator is fitted with a GTA welding head and weld camera. Olympus 5 MHz, 64 element phased array probes are used with high-temperature wedges and connected to a PEAK NDT Micropulse 6 controller. The weld bevel preparation is also shown with approximate pass structure. The passes relevant to experiments within this work are highlighted in red. (For interpretation of the references to colour in this figure legend, the reader is referred to the Web version of this article.)

3. Real-time weld pool monitoring

The next section documents the experimental procedure adopted to investigate phased array ultrasonic inspection to monitor the molten weld pool in various welding scenarios.

3.1. Experimental set-up

Fig. 3 shows the experimental hardware used. All welding trials were performed using a GTAW process, deployed via a Kuka KR-90 robotic arm. To monitor the weld deposition visually, a Xiris XVC-1000 High Dynamic Range (HDR) camera was used. The sample plates used were carbon steel S275 with dimensions of $100.0 \times 300.0 \times 15.8$ mm. The weld preparation was a single-V, 90° included bevel angle with a root gap of 2.0 mm and a root face of 1.5 mm.

The ultrasonic set-up was designed to provide longitudinal wave modes through the deposited weld in a pitch-catch arrangement as shown in **Fig. 4**. Longitudinal waves were chosen as they can be transmitted through molten material, unlike shear waves. Where solidification occurs, the faster speed of the longitudinal wave aids identification of the relevant signals as these are first to arrive. In previous literature [30], the use of both longitudinal and shear wave modes in both pitch-catch and pulse-echo arrangements for weld pool monitoring was documented with the longitudinal pitch-catch method providing the most useful results. It was therefore determined that a longitudinal pitch-catch approach should be adopted throughout these experiments. When planning the ultrasonic inspection, steps were taken to ensure that the ultrasonic hardware was suitably protected from the heat generated. This was achieved through the use of two Olympus 5L64-A32 probes with Olympus SA32-ULT-N55S-IHC high-temperature wedges enabling inspection up to 150 °C. The Probe Centre Separation (PCS) was chosen to be 112 mm, sufficient to allow travel of the weld torch between the wedges without collisions. To best account for the expected beam shifts due to temperature, an angular sweep from 75° to 80° with a fixed distance focus in x for all angles at the centreline of the weld preparation was implemented. In post-processing, the optimal angle could then be chosen based on the first arrival amplitude response. During all welding trials, the ultrasonic probes were fixed in position at the midpoint of the plate as shown in **Fig. 4b**, with the welding torch moving between them. The probes remaining static greatly simplifies the experimental hardware and procedures whilst still providing valuable results. The probes were clamped to the surface with a high-temperature liquid couplant to provide consistent acoustic coupling.

3.2. Welding experiments

Four targeted experiments were designed to specifically isolate and replicate common weld fabrication scenarios, namely:

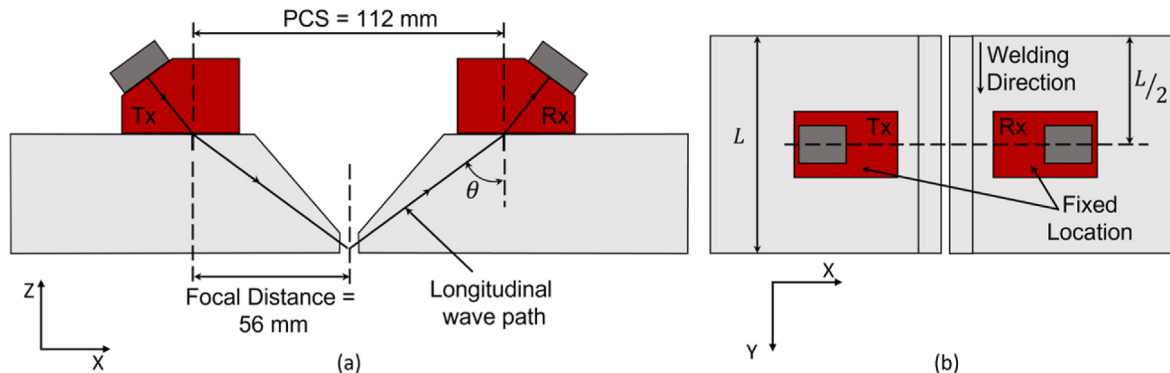


Fig. 4. Ultrasonic hardware set up and placement shown in (a) section view and (b) plan view. Highlighting Transmit (Tx) and Receive (Rx) probes, Probe Centre Separation (PCS) and focal distance.

- I. Bridging root weld to isolate the molten weld pool
- II. Full root weld replicating standard welding practice
- III. Full root weld with induced Lack of Root Penetration (LORP)
- IV. Short hot pass weld to isolate the molten weld pool in upper multi-pass layers

The welding parameters used were optimised over several separate trials not documented here. They are shown for each experiment in **Table 1**.

3.3. Experiment 1 – bridging root weld to isolate the molten weld pool

In the first instance, it was important to isolate the melt pool and observe the signal changes which occur when the welding arc is started and throughout the melting and solidification processes. To do this, the experiment began with a small solid tack weld placed in the centre of the two probes. **Fig. 5** shows a schematic diagram highlighting the position of the weld with respect to the ultrasonic probes. The welding arc was then ignited on top of this tack weld allowing a sufficient melt pool to be formed. This method restricts the acoustic transmission path initially through the solidified tack weld and then through the molten melt pool. Confirmation of the complete melting of this tack weld was provided visually through the Xiris weld camera. A short root weld of length 5 mm was then performed before the arc was extinguished and the weld was allowed to solidify and cool.

3.4. Experiment 1 - results & discussion

The angle chosen from the sectorial sweep was 75° focused at the centre point between the two probes as it provided the maximum amplitude without saturation occurring within the region of interest. The first signal arrival must contain only contributions from longitudinal waves without mode conversion. As it contains sufficient information to differentiate key characteristics of the weld pool it is the focus of the analysis. **Fig. 6a** shows a TOF map, displayed in the same style as a Time of Flight Diffraction (TOFD) B-scan. However, since the probes remain stationary throughout the experiment, the x-axis refers to acquisition time rather than the physical distance travelled. **Fig. 6b** shows individual A-scans each taken from key moments throughout the welding process as highlighted in **Fig. 6a**.

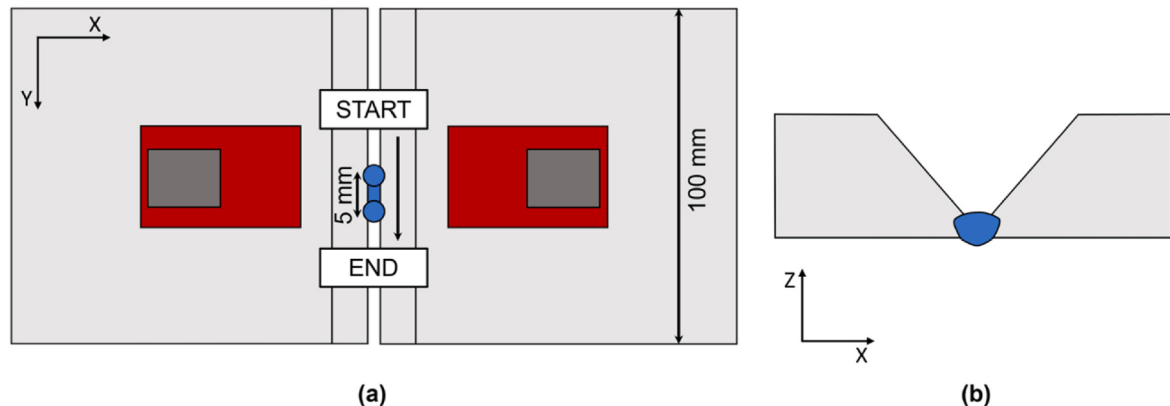
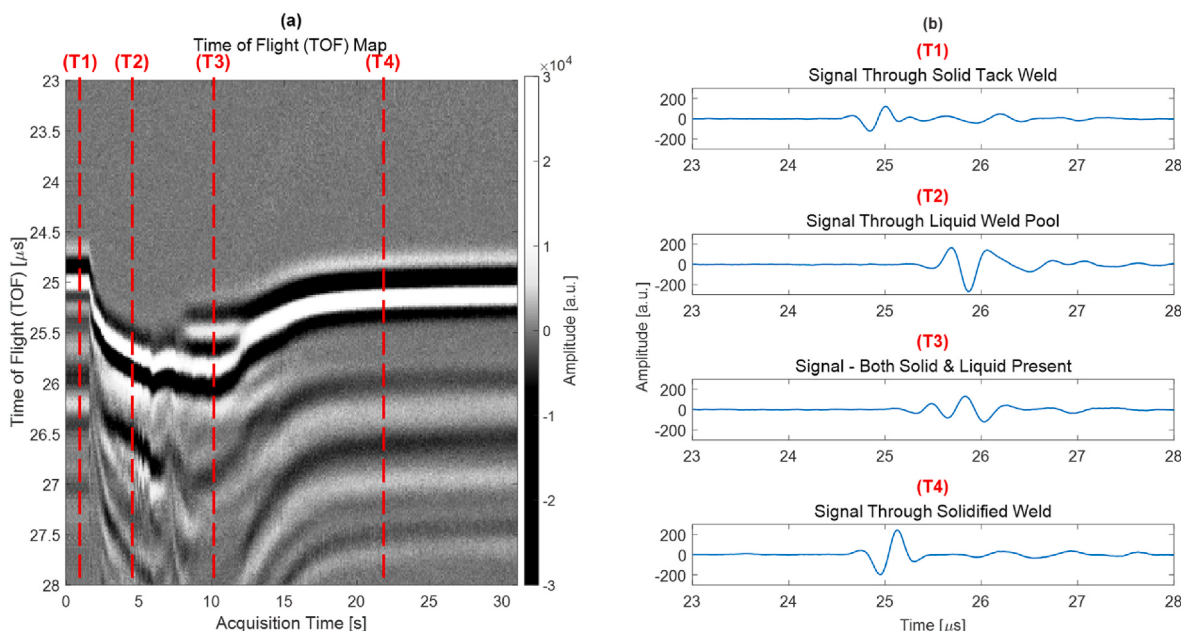
At T1 the ultrasonic beam is travelling through the solid tack weld at an ambient temperature of 22 °C. The signal has a positive phase, with the phase defined by the first peak amplitude of the signal, with a first arrival time of 24.7 μ s which is in agreement with a theoretical TOF calculation given the transmission angle, distance travelled in the wedges and PCS.

Between T1 and T2, the welding arc is ignited and the tack weld is melted. At this point, the ultrasonic beam path is restricted to travel

Table 1

Optimised welding parameters for each experiment.

Experiment Number	Sample Number	Pass	Current [A]	Arc Voltage [V]	Travel Speed [mm/min]	Wire Feed Speed [mm/min]	Weave Amplitude [mm]	Weave Frequency [Hz]
1	1	Root	135	12.5	50	1000	2.2	0.3
2	2	Root	135	12.5	50	1000	2.2	0.3
3	3	Root	135	12.5	50	1000	2.2	0.3
4	2	Hot	220	13	100	1225	4	0.6

**Fig. 5.** Schematic view of experiment 1 showing position of weld in relation to probes in both a (a) plan and (b) section view.**Fig. 6.** (a) Time of Flight (TOF) map of acquired ultrasonic signals (b) A-scans from highlighted acquisition times.

through the molten weld pool. Here, there is a clear TOF shift indicative of both the reduction in speed of sound associated with ultrasound travel through liquid and the extreme thermal gradients generated by the welding process. The signal also exhibits a 180° phase shift, now displaying a negative phase.

Between T2 and T3, the weld torch begins moving, performing a short 5 mm root weld. At time T3, an earlier arriving signal appears, indicating two ultrasonic paths being present with differing TOF's. While the use of 1D phased arrays provides accurate focusing in the X-Z plane, there is no lateral focusing capability in the X-Y plane. Now that the weld torch has moved, a shorter ultrasonic path is available through the already deposited and solidified portion of the weld, where the speed

of sound is faster. This shorter path is contained in the first peak of the signal. It is also noted that the signal has returned to having a positive phase, which is in agreement with the path of the earlier arriving signal being through solidified material. The second peak is seen to be continuous on the TOF map between T2 and T3, taking the reduced velocity path through the molten weld pool. The effect of the lateral beam spread is shown visually in Fig. 7a and related to the resultant ultrasonic signals at T3 through Fig. 7b.

As the arc is extinguished and the weld solidifies and cools, the signal through the liquid weld pool diminishes as the volume of accessible liquid reduces. The TOF reduces during this portion of the acquisition, which can be attributed to the cooling of the weld which would result in

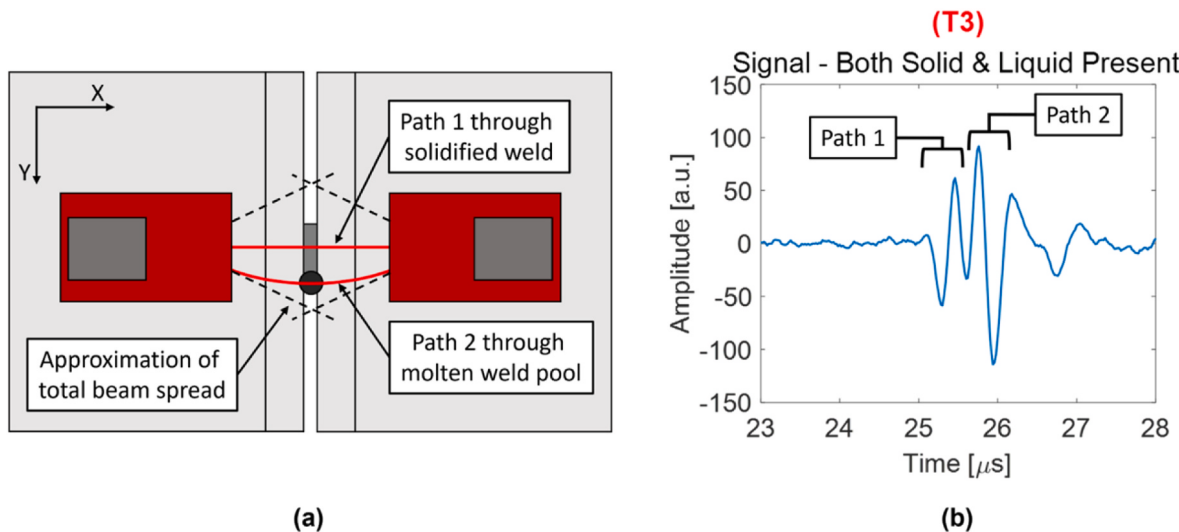


Fig. 7. Effects of lateral beam spread shown in (a) a plan view and linked to the resultant ultrasonic signals through (b).

an increase in wave velocity. Again, the signal through the solidified weld shows a positive phase.

A significant result here is the 180° phase shift displayed in the signal as the molten weld pool is established and then again as the weld solidifies. Ultrasonic phase changes are associated with a reflection from a high-to-low impedance boundary [41]. The reflection point in both the solid and liquid cases occurs at the base of the root and, with the assumption of a purely molten weld pool, the reflection interface in both cases is of high-to-low impedance (either solid steel-to-air, or molten steel-to-air). Therefore, the expectation is that both signals should contain the same phase, having both undergone the same phase reversal during their reflection. However, the results shown here indicate the opposite. One explanation for this, requiring further investigation, could be due to the lack of shielding gas present on the underside of the root allowing formation of an oxide layer [42]. Such a layer on the underside of the molten weld pool would change the reflection interface to being low-to-high (molten steel-to-oxide layer), resulting in the ultrasonic wave no longer experiencing a phase reversal.

These results show that real-time weld pool monitoring through ultrasonic means is possible. Focused longitudinal ultrasonic waves have been successfully transmitted through the molten weld pool with the received signals containing significant information relating to the physical state of the weld material. By recording changes in these signals and recognising the appropriate features within the signal, such as phase

and TOF, it is possible to monitor the weld pool directly.

3.5. Experiment 2 – full root pass weld replicating standard welding practice

The next experiment looks to observe if these same signal changes are visible when depositing a full root pass weld past the stationary probes. Here, the weld is initiated at one end of the plate outside of the lateral beam spread of the probes. The weld then transits between the two probes and ends at the opposite end of the plate, with a total weld length of 90 mm. **Fig. 8** shows a schematic diagram highlighting the position of the weld with respect to the ultrasonic probes.

3.6. Experiment 2 - results and discussion

The angle chosen from the sectorial sweep was 75° focused at the centre point of the two plates as it provided the maximum amplitude without saturation occurring within the region of interest. **Fig. 9a** shows the TOF map created during this experiment, with key A-scans taken from highlighted points during the welding and acquisition shown in **Fig. 9b**. Initially, there is no material between the plates for sound to be transmitted and therefore there is no signal visible. As previously discussed, there is no focusing capability in the X-Y plane and consequently, the initial signal through the molten weld pool is visible before

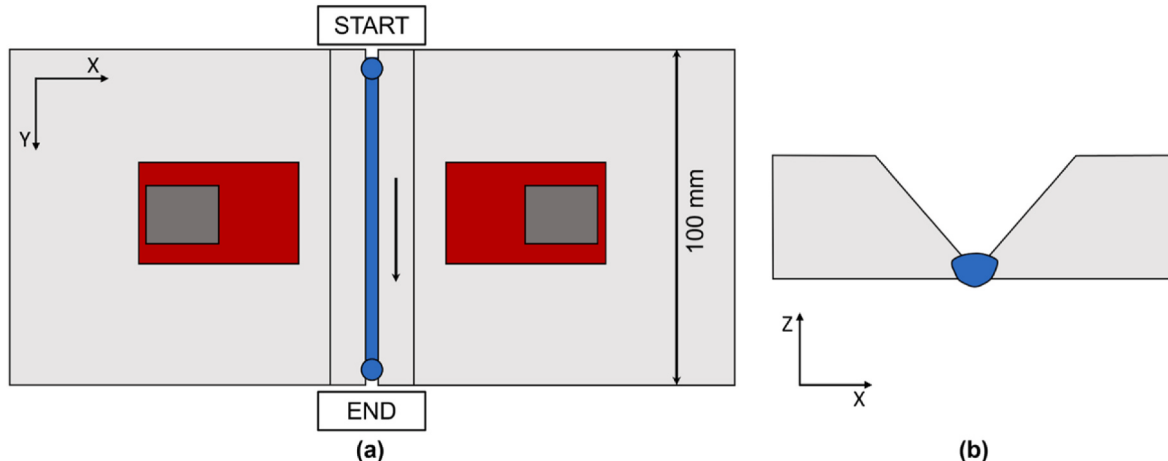


Fig. 8. Schematic view of experiment 2 showing position of weld in relation to probes in both a (a) plan and (b) section view.

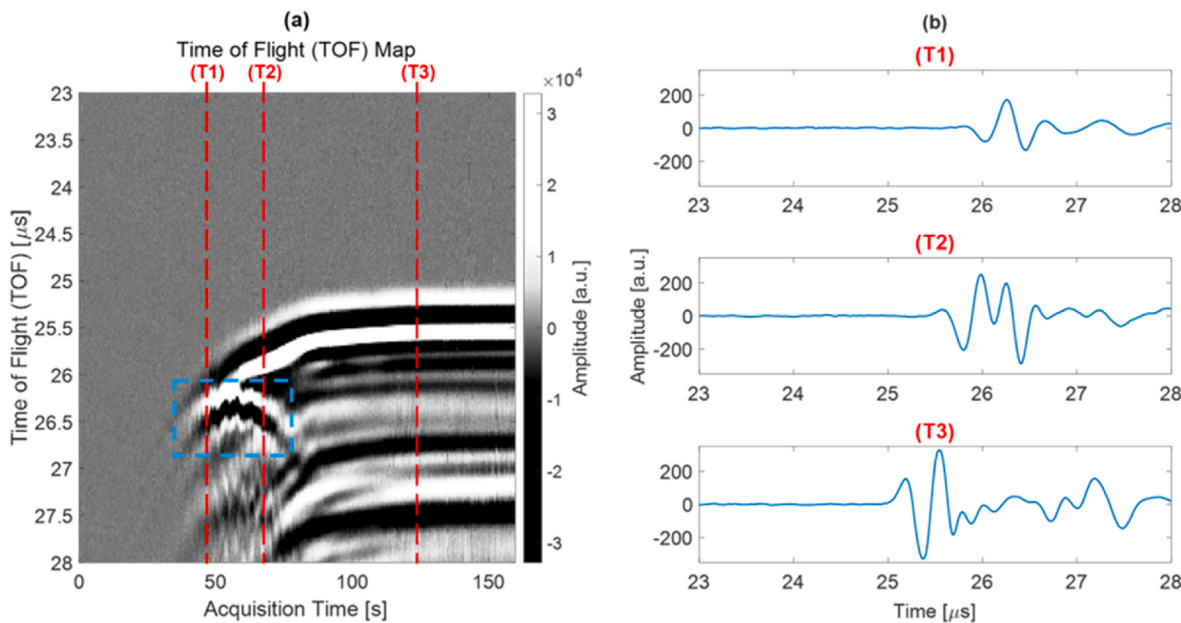


Fig. 9. (a) Time of Flight (TOF) map of acquired ultrasonic signals (b) A-scans from highlighted acquisition times.

the weld reaches the midpoint of the probes. At the highlighted acquisition time, T1, the emerging molten weld pool is located at the outer edges of the beam spread and therefore is lower in amplitude due to reduced beam energy. It does show the same characteristic negative phase cycle as observed in Section 3.4. The parabolic shape created in the TOF map highlighted by the blue dotted box in Fig. 9a is indicative of the molten weld pool passing across the beam spread of the probes. This changing TOF gives the illusion of varying wave speed, however, this is actually due to the change in path length. This effect is shown visually in Fig. 10.

The ultrasonic path length through the molten weld pool is minimised at point 2 in Fig. 10 and maximised at the outer extremities of the beam spread at points 1 and 3. Therefore the TOF will minimise and maximise as the molten weld pool passes across the beam spread, creating this distinctive parabolic shape as shown in Fig. 10b.

At time T2 in Fig. 9a, the signal is seen to divide, again this is suggestive of there being two ultrasonic paths available. This is in

agreement with the results shown in Section 3.4, where the first peak is attributed to the faster path through the already deposited and solidified weld and the second to the path through the molten weld pool. Finally, as the molten weld pool moves outside of the beam spread of the probes again, the second peak diminishes in size leaving only the signal through the solidified weld. This signal again displays a positive wave cycle and its TOF reduces as the weld cools and the wave speed increases as a consequence.

These results show that it is possible to identify the longitudinal wave mode transmitted through the liquid weld pool and to track its movement across the beam spread of the probes. It also shows that the same characteristic signal features are present within the received signal, such as phase reversal, TOF changes and signal division.

3.7. Experiment 3 – full root weld with induced Lack of Root Penetration

Here, an embedded tungsten tube (ID 1.5 mm, OD 3.0 mm) was used

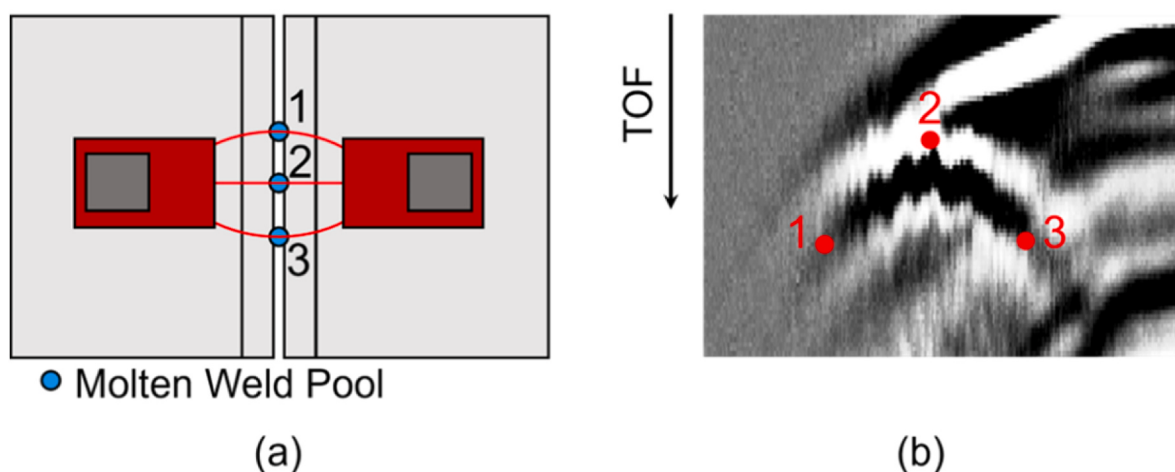


Fig. 10. (a) Diagram showing changing path length as weld transits across probe beam spread. (b) Highlighted in TOF map.

to induce extensive Lack of Root Penetration (LORP). Embedded tungsten rods and tubes have been used widely in the past to simulate various types of defects [43,44]. The tungsten tube was manually tacked into position at the centre of the probes and at the base of the root in order to prevent the melt pool from fusing to either root face. All deposited material will be on top of the tungsten tube. Fig. 11 shows a schematic diagram highlighting the position of the tungsten tube with respect to the ultrasonic probes.

3.8. Experiment 3 - results & discussion

Fig. 12a shows the underside of the weld performed in Experiment 1, Section 3.3, which displays consistent root penetration compared with the resultant LORP achieved using the tungsten tube barrier shown in Fig. 12b. This method of adding a tungsten tube was deemed successful at simulating LORP. The angle selected from the sectorial sweep was 75°, therefore the results are directly comparable with those shown for Experiment 1 in Section 3.4.

The TOF maps for both welds are shown in Fig. 13. The parabolic portion, highlighted as a blue dotted box in both TOF maps, indicates the time period when the molten weld pool is located within the probes beam spread. It can be seen that while the parabolic shape is clear and uninterrupted in Fig. 13a, it is no longer continuous in Fig. 13b. The variation in the signal pattern visible here indicates a change in the ultrasonic path between the two probes caused by the introduction of LORP. This suggests that the proposed weld monitoring method explored here can successfully distinguish between good and poor root weld penetration.

There is a difference in the TOF between Fig. 13a and b for the signal through the final solidified weld. As there was no alteration to the welding process to induce the LORP, the volume of deposited material is the same in both cases, however, the tungsten tube barrier causes the weld volume to sit higher up the weld groove. As visible in Fig. 1b, the beam focusing does not provide an absolute pin-point focal spot but rather a concentration of energy. This means that some ultrasound will be able to transmit across the deposited material above the tungsten, however, it will have a reduced path length resulting in a shorter TOF.

3.9. Experiment 4 – short hot pass weld to isolate molten weld pool in upper multi-pass layers

As previously discussed in Section 2.1, the use of phased arrays enables the concentration of ultrasonic energy to maximise the transmission through any given point. Therefore, it is possible to isolate individual passes with more accuracy than would be possible with single-element inspection systems. To investigate this, an experiment

was developed to isolate the molten weld pool during the deposition of the hot pass, or second layer, of a multi-pass weld. The welded sample produced in Section 3.3 with an already-deposited root pass was used and a short hot pass was performed on top of it. The hot pass was ignited between the two probes and the weld pool was allowed to grow in size before a short 10 mm length weld was performed as shown in the schematic of Fig. 14.

3.10. Experiment 4 - results & discussion

The angle of inspection chosen was 80°, as this provided a suitable amplitude response without saturation within the region of interest. The signal highlighted in Fig. 15a and b as T1 is known to be travelling through the already deposited, room-temperature root pass. As expected, this signal shows a positive phase cycle. At an acquisition time of 22.5 s, the arc is ignited and the signal immediately divides as shown in the highlighted signal T2. Since there is surrounding solidified material present both below the hot pass and immediately before and after the arc-ignition position, there will always be two paths for the ultrasound to take. Again, these two paths can be identified in the divided signals due to their associated differing acoustic velocities. The TOF shift visible between T1 and T2 is due to the temperature gradient induced by the welding process. As the arc is extinguished and the weld begins to cool, the two peaks re-join and a single signal is seen in T3 representing the signal through the solidified material.

These results indicate that through appropriate focusing and steering of ultrasound through the use of phased arrays it is possible to successfully isolate signals transmitted through the molten weld pool within various layers in a multi-pass weld.

4. Future work

The primary limitation of this proposed monitoring technique is the fixed location of the ultrasonic probes. In order to make this approach more practical, scanning of the probes in-line with the weld torch is necessary for providing continuous monitoring. Capturing data at specified increments would provide an encoded record of the welding process with positional data provided through robotic deployment. Furthermore, concurrent monitoring will be better suited to analysing signal changes which may indicate the formation of various defects and how these may relate to changes in the welding process. The use of a weld inspection roller probe [40] would allow for smooth robotic translation of the probes whilst maintaining consistent coupling.

Another constraint upon future deployment is the use of liquid coupling which could cause contamination of the weld when combined with the movement of the probes, resulting in defects such as gross

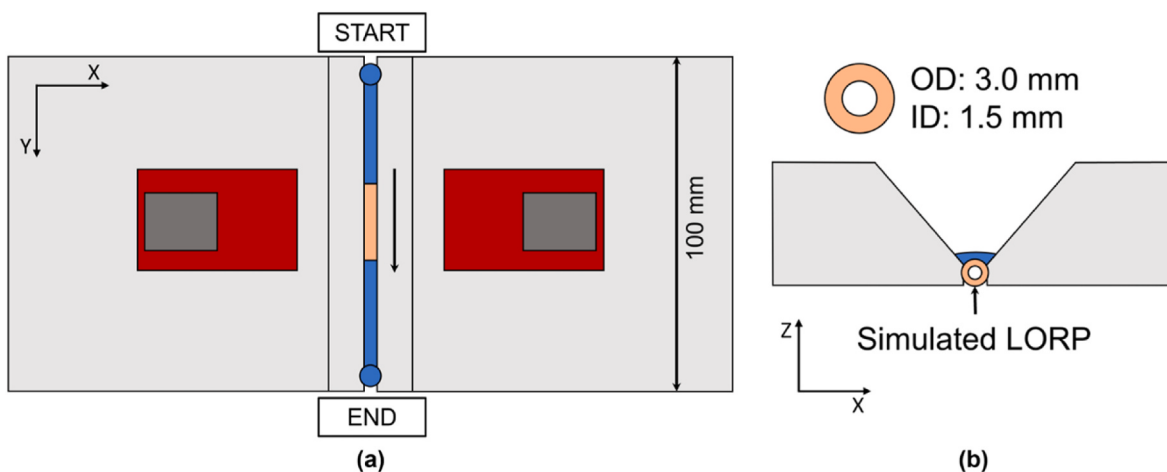


Fig. 11. Schematic view of experiment 3 showing position of weld in relation to probes in both a (a) plan and (b) section view.

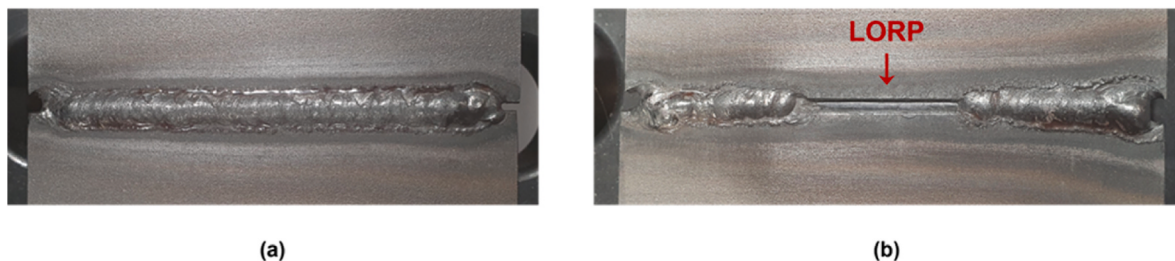


Fig. 12. Photographs of the underside of root welds showing (a) consistent root penetration and (b) induced Lack of Root Penetration (LORP).

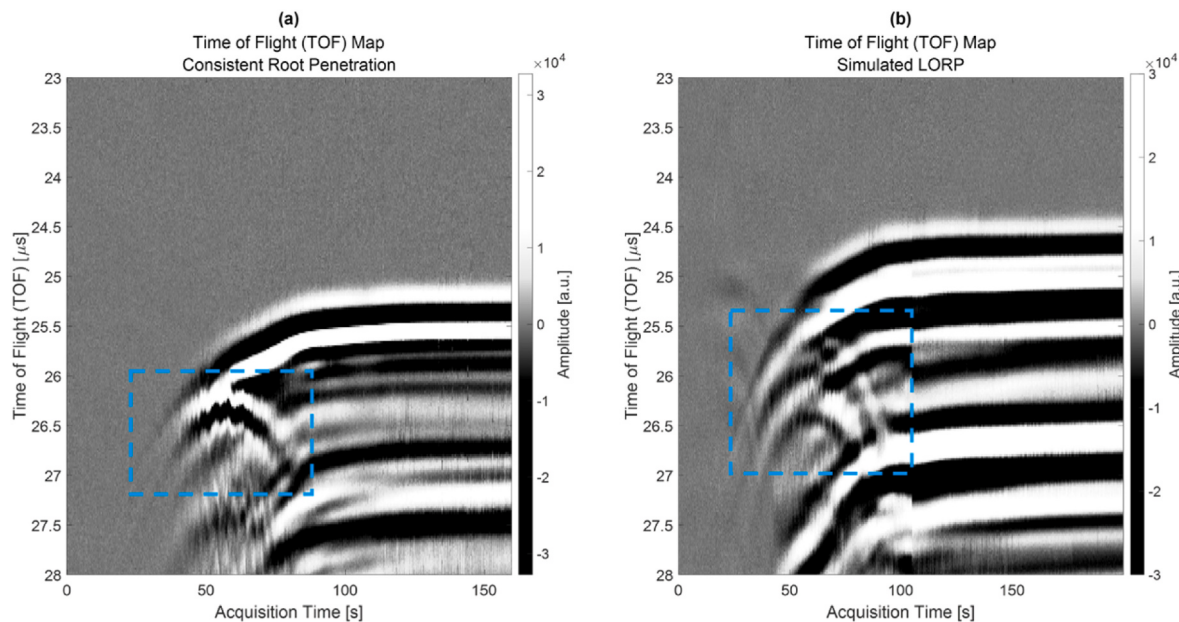


Fig. 13. TOF maps for (a) experiment 1 with consistent root penetration and (b) experiment 3 with Lack of Root Penetration (LORP) present.

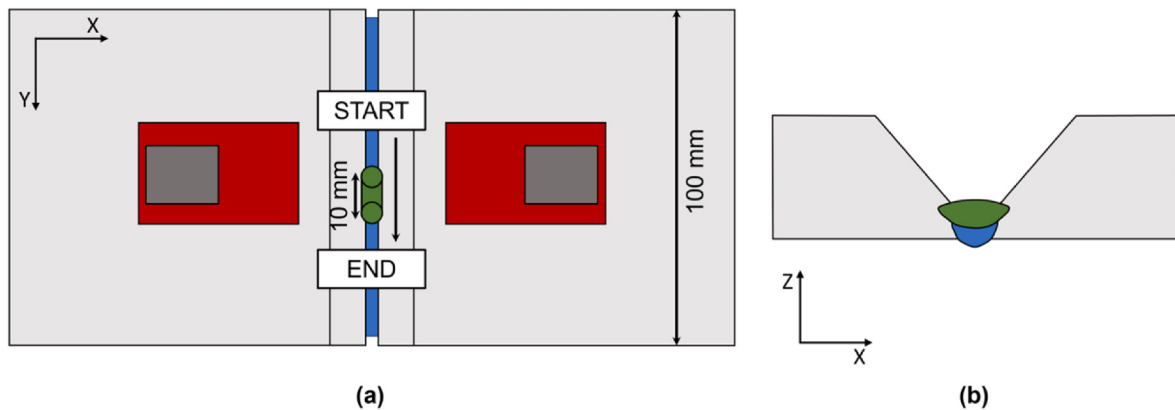


Fig. 14. Schematic view of experiment 4 showing position of weld in relation to probes in both a (a) plan and (b) section view.

porosity. Dry-coupling techniques which use high-temperature polymers with optimised acoustical properties are a promising method to enable couplant-free deployment.

The experiments documented here are focused on the monitoring of the root and hot passes, however, with suitable modifications made to the ultrasonic focusing and deployment, the same technique may be used to monitor higher passes within multi-pass welding. Furthermore, this technique will also be applicable to welding processes other than GTAW such as Gas Metal Arc Welding (GMAW) and SAW.

The results shown here indicate considerable promise for

quantitative analysis of the weld pool size using the TOF data contained within the ultrasonic signals. This direction of research would provide a significant step forward in progress towards automated control of the welding process using ultrasonics. This work requires accurate knowledge of the weld pool temperature and consequent speed of sound to provide accurate measurements. Currently, the available data on temperature vs. speed of ultrasonic waves is limited to 1100 °C [45] and future work is being undertaken to understand and quantify this variation.

Further investigation is also required to accurately identify the

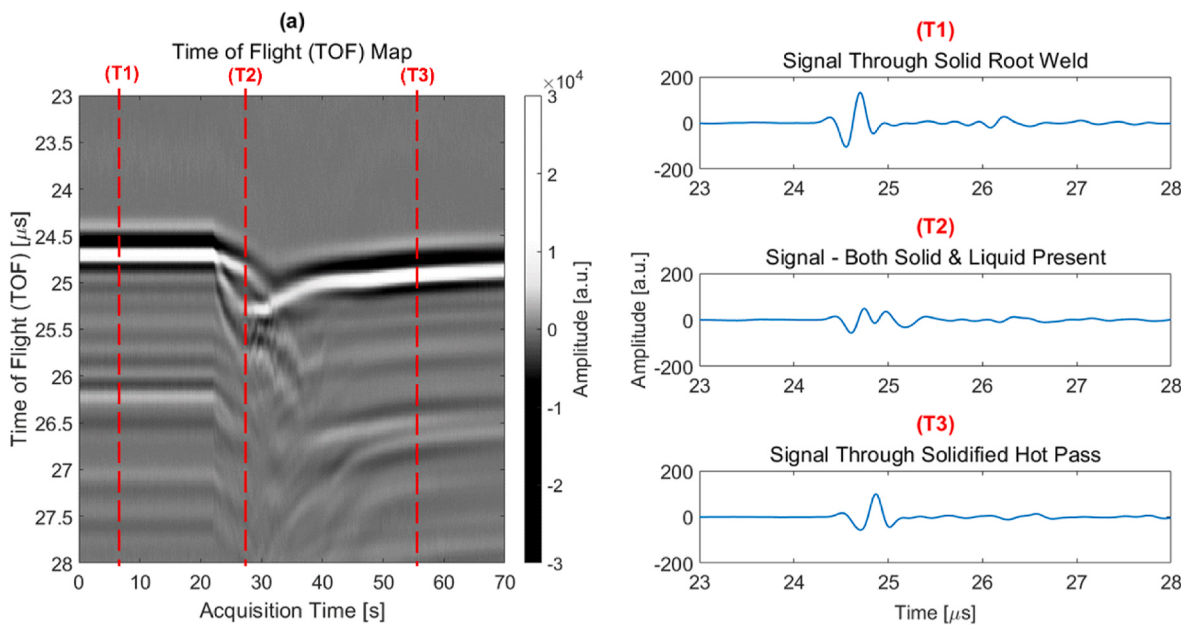


Fig. 15. (a) Time of Flight (TOF) map of acquired ultrasonic signals (b) A-scans from highlighted acquisition times.

physical mechanism which results in the 180° phase reversal observed between signals through solidified weld material and the molten weld pool.

5. Conclusions

In-process phased array monitoring of welding processes offers significant technical and commercial benefits to the future of manufacturing. In the work reported here, focused phased array pitch-catch inspection techniques have been implemented successfully for in-process monitoring of both root and hot pass gas tungsten arc welds. It has been proven that despite the harsh environment that welding presents, ultrasonic waves can be propagated successfully through the molten weld pool. The resultant signals have been analysed and found to contain significant information relating to physical changes taking place within the welding process, namely the transition from solid weldment to a molten weld pool, and back again. These signal changes have been shown to be useful in determining weld quality with notable variations occurring when defects such as LORP are present. It is believed that with modification to the deployment strategy to allow for in-line, concurrent inspection, the signal responses are of sufficient quality that they offer a significant opportunity to form the basis of a closed-loop control system in the future.

Author statement

Nina E. Sweeney: Conceptualization, Methodology, Investigation, Formal Analysis, Writing – Original Draft.

Simon Parke: Supervision, Writing – Review & Editing.

David Lines: Software, Writing – Review & Editing.

Charalampos Loukas Software.

Momchil Vasilev Software.

Gareth Pierce: Supervision, Writing – Review & Editing.

Charles N. MacLeod: Supervision, Methodology, Writing – Review & Editing.

Funding

The author acknowledges the funding of the Research Centre for Non-Destructive Evaluation (RCNDE) on behalf of Peak NDT Ltd

through the Engineering and Physical Sciences Research Council (EPSRC) Centre for Doctoral Training in Future Innovation in Non-Destructive Evaluation (EP/S023275/1).

Declaration of competing interest

The authors declare that they have no known competing financial interests or personal relationships that could have appeared to influence the work reported in this paper.

Data availability

Data will be made available on request.

Appendix A. Supplementary data

Supplementary data to this article can be found online at <https://doi.org/10.1016/j.ndteint.2023.102850>.

References

- [1] The British Standards Limited. BS EN ISO 17640:2018: non-destructive testing of welds. Ultrasonic testing. Techniques, testing levels, and assessment. 2019. 2019.
- [2] The British Standards Limited. BS EN ISO 19285:2017: non-destructive testing of welds. Phased array ultrasonic testing (PAUT). Acceptance levels. 2017. 2017.
- [3] International Energy Agency, IEA. Net zero by 2050 - a roadmap for the global energy sector. n.d.
- [4] Cheng Y, Yu R, Zhou Q, Chen H, Yuan W, Zhang Y. Real-time sensing of gas metal arc welding process – a literature review and analysis. J Manuf Process 2021;70: 452–69. <https://doi.org/10.1016/j.jmapro.2021.08.058>.
- [5] Li X, Li X, Ge SS, Khyam MO, Luo C. Automatic welding seam tracking and identification. IEEE Trans Ind Electron 2017;64:7261–71. <https://doi.org/10.1109/TIE.2017.2694399>.
- [6] Muhammad J, Altun H, Abo-Serie E. Welding seam profiling techniques based on active vision sensing for intelligent robotic welding. Int J Adv Manuf Technol 2017; 88:127–45. <https://doi.org/10.1007/s00170-016-8707-0>.
- [7] Zhang YM. Part 2 chapter 6: weld seam monitoring. Real-time weld process monitoring. Elsevier; 2008. p. 129–86.
- [8] Le J, Zhang H, Chen X. Right-angle fillet weld tracking by robots based on rotating arc sensors in GMAW. Int J Adv Manuf Technol 2017;93:605–16. <https://doi.org/10.1007/s00170-017-0536-2>.
- [9] Font comas T, Diao C, Ding J, Williams S, Zhao Y. A passive imaging system for geometry measurement for the plasma Arc Welding process. IEEE Trans Ind Electron 2017;64:7201–9. <https://doi.org/10.1109/TIE.2017.2686349>.
- [10] Peng G, Chang B, Wang G, Gao Y, Hou R, Wang S, et al. Vision sensing and feedback control of weld penetration in helium arc welding process. J Manuf Process 2021;72:168–78. <https://doi.org/10.1016/j.jmapro.2021.10.023>.

- [11] Brzakovic D, Khani DT, Awad B. A vision system for monitoring weld pool. In: Proceedings 1992 IEEE international conference on robotics and automation, vol. 2; 1992. p. 1609–14. <https://doi.org/10.1109/ROBOT.1992.220022>.
- [12] Chen Z, Chen J, Feng Z. Welding penetration prediction with passive vision system. *J Manuf Process* 2018;36:224–30. <https://doi.org/10.1016/j.jmapro.2018.10.009>.
- [13] Alfaro SCA, Franco FD. Exploring infrared sensoring for real time welding defects monitoring in GTAW. *Sensors* 2010;10:5962–74. <https://doi.org/10.3390/s100605962>.
- [14] Bicknell A, Smith JS, Lucas J. Infrared sensor for top face monitoring of weld pools. *Meas Sci Technol* 1994;5:371–8. <https://doi.org/10.1088/0957-0233/5/4/008>.
- [15] The British Standards Limited 2013. BS EN ISO 5579:2013: non-Destructive Testing - Radiographic testing of metallic materials using film and X- or gamma rays - basic Rules. 2013.
- [16] Health and Safety Executive (HSE). L121 work with ionising radiation: ionising radiations regulations 2017. Approved code of practice and guidance. second ed. TSO (The Stationery Office); 2018.
- [17] Shull PJ. Theory, techniques, and applications. Boca Raton: CRC Press; 2016. p. 108. <https://doi.org/10.1201/9780203911068> [Chapter 5]: Eddy Current.
- [18] Maev RG, Chertov AM, Paille JM, Ewaszyn FJ. Ultrasonic in-process monitoring and feedback of resistance spot weld quality. US20170021446A1; 2017.
- [19] Maev R, Chertov A, Regaldo W, Karloff A, Tchipilko A, Lichaa P, et al. In-line inspection of resistance spot welds for sheet metal assembly. *Weld J* 2014;93: 58–62.
- [20] Andreoli AF, Chertov AM, Maev RG. Correlation between peel test and real time ultrasonic test for quality diagnosis in resistance spot welding. *Soldag Insp* 2016; 21:282–9. <https://doi.org/10.1590/0104-9224/SI2103.04>.
- [21] Stocco D, Maev RG, Chertov AM, Batalha GF. Comparison between in-line ultrasonic monitoring of the spot weld quality and conventional NDT methods applied in a real production environment. *e-J Non-Destruc Test* 2008;Vol. 13(11). <https://www.ndt.net/?id=6496>.
- [22] Lui A, Karloff AC, Rgr Maev. M-scan cross-sectional imaging of resistance spot welds during welding. *IEEE International Ultrasonics Symposium*; 2012. p. 2392–5. <https://doi.org/10.1109/ULTSYM.2012.0598>. 2012.
- [23] Lui A, Karloff AC, Chertov AM, Rgr Maev, Boni E, Tortoli P. Application of a programmable multi-channel ultrasonic system for in-line quality monitoring of spot welds. In: 2011 IEEE international ultrasonics symposium; 2011. p. 524–6. <https://doi.org/10.1109/ULTSYM.2011.0126>.
- [24] Vasilev M, MacLeod C, Galbraith W, Javadi Y, Foster E, Dobie G, et al. Non-contact in-process ultrasonic screening of thin fusion welded joints. *J Manuf Process* 2021; 64:445–54. <https://doi.org/10.1016/j.jmapro.2021.01.033>.
- [25] Kelly SP, Farlow R, Hayward G. Applications of through-air ultrasound for rapid NDE scanning in the aerospace industry. *IEEE Trans Ultrason Ferroelectrics Freq Control* 1996;43:581–91. <https://doi.org/10.1109/58.503780>.
- [26] Nomura K, Deno S, Matsuda T, Otaki S, Asai S. In situ measurement of ultrasonic behavior during lap spot welding with laser ultrasonic method. *NDT E Int* 2022; 130:102662. <https://doi.org/10.1016/j.ndteint.2022.102662>.
- [27] Mi B, Ume C. Real-time weld penetration depth monitoring with laser ultrasonic sensing system. *J Manuf Sci Eng* 2005;128:280–6. <https://doi.org/10.1115/1.2137747>.
- [28] Cerniglia D, Montinaro N. Defect detection in additively manufactured components: laser ultrasound and laser thermography comparison. *Procedia Struct Integr* 2018;8:154–62. <https://doi.org/10.1016/j.prostr.2017.12.016>.
- [29] Vasilev M, MacLeod C, Javadi Y, Pierce G, Gachagan A. Feed forward control of welding process parameters through on-line ultrasonic thickness measurement. *J Manuf Process* 2021;64:576–84. <https://doi.org/10.1016/j.jmapro.2021.02.005>.
- [30] Stares IJ, Duffil C, Ogilvy JA, Scruby CB. On-line weld pool monitoring and defect detection using ultrasonic. *NDT E Int* 1990;23:195–200. [https://doi.org/10.1016/0308-9126\(90\)91601-O](https://doi.org/10.1016/0308-9126(90)91601-O).
- [31] Halmshaw R. 4.2 waves at boundaries. *Non-Destructive testing*. second ed. London: E. Arnold; 1991. p. 106–23.
- [32] Drinkwater BW, Wilcox PD. Ultrasonic arrays for non-destructive evaluation: a review. *NDT E Int* 2006;39:525–41. <https://doi.org/10.1016/j.ndteint.2006.03.006>.
- [33] Clay AC, Wooh S-C, Azar L, Wang J-Y. Experimental study of phased array beam steering characteristics. *J Nondestr Eval* 1999;18:59–71. <https://doi.org/10.1023/A:1022618321612>.
- [34] EXTEnde. CIVA NDE software manual. 2020.
- [35] Scruby CB, Moss BC. Non-contact ultrasonic measurements on steel at elevated temperatures. *NDT E Int* 1993;26:177–88. [https://doi.org/10.1016/0963-8695\(93\)90427-2](https://doi.org/10.1016/0963-8695(93)90427-2).
- [36] Silber FA, Ganglbauer C. Ultrasonic testing of hot welds. *Non-Destr Test* 1970;3: 429–32. [https://doi.org/10.1016/0029-1021\(70\)90156-8](https://doi.org/10.1016/0029-1021(70)90156-8).
- [37] Javadi Y, Mohseni E, MacLeod CN, Lines D, Vasilev M, Mineo C, et al. Continuous monitoring of an intentionally-manufactured crack using an automated welding and in-process inspection system. *Mater Des* 2020;191:108655. <https://doi.org/10.1016/j.matdes.2020.108655>.
- [38] Mineo C, Lines D, Cerniglia D. Generalised bisection method for optimum ultrasonic ray tracing and focusing in multi-layered structures. *Ultrasonics* 2021; 111:106330. <https://doi.org/10.1016/j.ultras.2020.106330>.
- [39] Kirk KJ, McNab A, Cochram A, Hall I, Hayward G. Ultrasonic arrays for monitoring cracks in an industrial plant at high temperatures. *IEEE Trans Ultrason Ferroelectrics Freq Control* 1999;46:311–9. <https://doi.org/10.1109/58.753019>.
- [40] Vithanage RKW, Mohseni E, Qiu Z, MacLeod C, Javadi Y, Sweeney N, et al. A phased array ultrasound roller probe for automated in-process/interpass inspection of multipass welds. *IEEE Trans Ind Electron* 2020. <https://doi.org/10.1109/TIE.2020.3042112>. 1–1.
- [41] Krautkrämer J, Krautkrämer H. *Plane sound waves at boundaries*. *Ultrasonic testing of materials*. Springer Science & Business Media; 2013. p. 23–45.
- [42] Mills KC, Keene BJ. Factors affecting variable weld penetration. *Int Mater Rev* 1990;35:185–216. <https://doi.org/10.1179/095066090790323966>.
- [43] Mohseni E, Javadi Y, Sweeney NE, Lines D, MacLeod CN, Vithanage RKW, et al. Model-assisted ultrasonic calibration using intentionally embedded defects for in-process weld inspection. *Mater Des* 2021;198. <https://doi.org/10.1016/j.matdes.2020.109330>.
- [44] Javadi Y, Sweeney NE, Mohseni E, MacLeod CN, Lines D, Vasilev M, et al. In-process calibration of a non-destructive testing system used for in-process inspection of multi-pass welding. *Mater Des* 2020;195:108981. <https://doi.org/10.1016/j.matdes.2020.108981>.
- [45] Foster EA, Sweeney NE, Nicolson E, Singh J, Rizwan MK, Lines D, et al. Thermal compensation of ultrasonic transmit and receive data for steel welded plates at the point of manufacture. *NDT E Int* 2023;137:102812. <https://doi.org/10.1016/j.ndteint.2023.102812>.